Second-day road log from Las Cruces to Selden Canyon, Broad Canyon, and Rincon Arroyo

Greg H. Mack and Nancy J. McMillan
1998, pp. 23-34. https://doi.org/10.56577/FFC-49.23

in:

Las Cruces Country II, Mack, G. H.; Austin, G. S.; Barker, J. M.; [eds.], New Mexico Geological Society 49th Annual Fall Field Conference Guidebook, 325 p. https://doi.org/10.56577/FFC-49

This page is intentionally left blank to maintain order of facing pages.

SECOND-DAY ROAD LOG FROM LAS CRUCES TO SELDEN CANYON, BROAD CANYON, AND RINCON ARROYO

GREG H. MACK and NANCY J. McMILLAN

FRIDAY, NOVEMBER 6, 1998

Assembly point: Days Inn parking lot, corner of University Avenue and Main Street, Las Cruces. Take University Avenue east to junction with I-25. Go north on I-25, following First-day Road Log. Take exit 19—Radium Springs—and turn left at stop sign. Second-day road log begins here.

Departure time: 8:00 a.m.

Distance: 60 mi

Stops: 3 with 6 foot-log stops

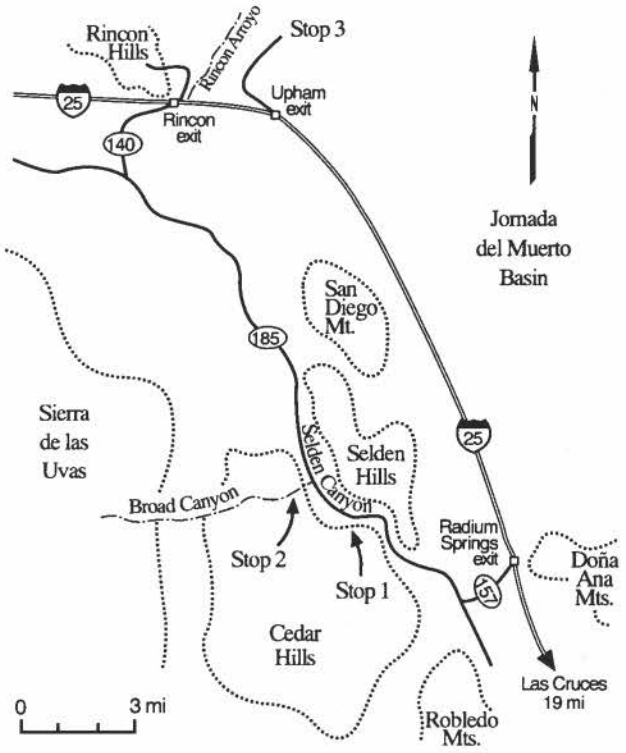

Summary

The second day of the field conference is dedicated to the Cenozoic history of southern New Mexico exposed in Selden Canyon, Broad Canyon, and near Rincon. The first stop in Selden Canyon is a roadcut of the late Eocene Palm Park Formation, which consists of very coarse-grained andesitic lahars. The Palm Park Formation represents volcanism that immediately preceded the onset of crustal extension of the Rio Grande rift and post-dated Laramide shortening. The second stop is a long traverse up Broad Canyon to examine Oligocene and Miocene rocks that formed during the early evolution of the Rio Grande rift. Stratigraphic units encountered include the early Oligocene Bell Top Formation, the late Oligocene Uvas Basaltic Andesite (including part of a cinder cone), and the late Miocene Rincon Valley Formation, including the 9.6 Ma Selden Basalt. These rocks are exposed in the Cedar Hills transfer zone, which is between the west Robledo Mountains fault and the Ward Tank fault (Mack and Seager, 1995). Two of the normal faults within the transfer zone can be observed on the traverse. The Broad Canyon traverse ends with a view of Native American petroglyphs etched into ash-flow tuff 5 of the Bell Top Formation (Seager et al., l975). The third stop is in a tributary canyon to Rincon Arroyo, where the axial-fluvial lithofacies of the Plio–Pleistocene Camp Rice Formation is exposed beneath the La Mesa geomorphic surface. Important features at this stop include the stage V petrocalcic paleosol beneath the La Mesa surface (Gile et al., 1981), calcic paleosols within the Camp Rice Formation (Mack and James, 1992), and a pumice-clast conglomerate within the Camp Rice Formation derived from the lower Bandelier eruption in the Jemez volcanic field (Mack et al., 1996). In addition, age dating and correlation of the Camp Rice Formation using reversal magnetostratigraphy will be discussed (Mack et al., 1993).

Mileage

Follow first-day road log from Las Cruces to Radium Springs exit of I-25.

0.0 **Exit I-25** at Radium Springs (exit 19). **Turn left** at stop sign onto NM-157 (Fort Selden Road). **0.7**

0.7 Cross railroad tracks. Road is on the Leasburg geomorphic surface (Gile et al., 1981). **0.7**

1.4 Pass entrance to Fort Selden. **0.2**

1.6 T-junction. **Turn right** onto NM-185. **0.3**

1.9 The highway crosses the Rio Grande. **0.7**

2.6 Enter the town of Radium Springs. **0.2**

2.8 Blue Moon Bar at 3:00. Outcrop across from bar is composed of late Pleistocene inset gravel. **0.5**

3.3 Junction with Faulkner Canyon Road. **Proceed north on NM-185. 2.7**

6.0 **STOP 1** at pullout on southwest side of road (Figs. 2.1 and 2.2). Exposed here is the late Eocene Palm Park Formation, which consists of coarse-grained andesitic lahars. The Palm Park and correlative Rubio Peak Formations record a major calc-alkaline magmatic episode throughout southern New Mexico. Post-Laramide volcanism deposited a blanket of volcaniclastic debris across southern New Mexico that is dominated by lahars, sandstones, and conglomerates intercalated with lava flows and tuffs. Three volcanic centers of this age have been identified in south-central New Mexico by the presence of near-vent volcanic facies or hypabyssal intrusions: Rubio Peak lavas in the southern Cooke's Range (Seager et al., 1982) and in the Good Sight Mountains (Clemons, 1979), and the Cleofas hypabyssal intrusion in the Doña Ana Mountains (Seager et al., 1976). However, the locations of volcanic centers that produced specific volcaniclastic units are equivocal because of the difficulty of determining paleocurrent directions in lahars and correlation of individual units across fault blocks. Ramirez et al. (1995) compared the major and trace element compositions of volcanic casts in lahars from three sections in the Palm Park and Rubio Peak Formations (southern Cooke's Range, Faulkner

FIGURE 2.1. Stop 1, NM-185 roadcut of the Eocene Palm Park Formation.

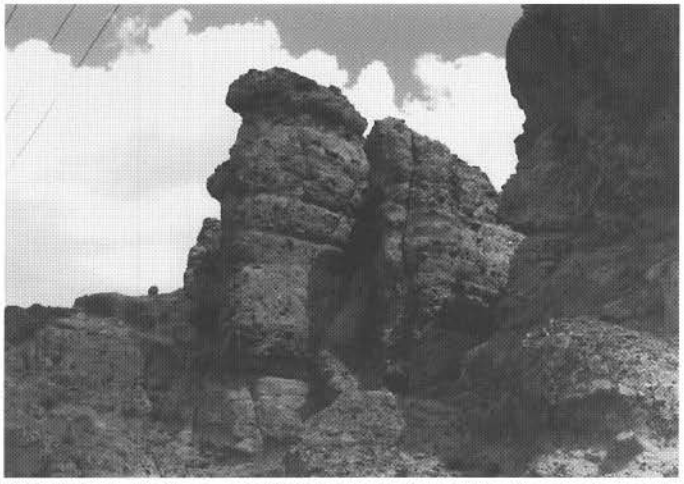

FIGURE 2.2. Medium- and thick-bedded lahars of the Eocene Palm Park Formation at Stop 1.

FIGURE 2.3. View of the late Miocene Selden Basalt from NM-185.

Canyon, East Selden Hills) with the in situ lavas and intrusions as a method of correlating volcanic aprons to volcanic centers. Because the three volcaniclastic sections have distinct concentrations of immobile incompatible trace elements, the sections appear to have originated from three separate vents. Lavas from the Cooke's Range and Good Sight Mountains have higher Y and Zr than any of the suites of lahar clasts, precluding them as volcanic centers for the lahars. However, the Cleofas intrusion is similar in composition to clasts from the East Selden Hills and Faulkner Canyon, and is probably the volcanic center for one or both of these lahar suites. **0.5**

6.5 Highway is on the floodplain of the Rio Grande. Cliffs at 9:00 are composed of the late Miocene Rincon Valley Formation, which consists of red conglomerates and the 9.6 Ma Selden Basalt (Fig. 2.3). **0.8**

7.3 At 9:00 is exposure of the Selden Hills fault that juxtaposes red pebble conglomerate of the late Miocene Rincon Valley Formation and the late Oligocene Uvas Basaltic Andesite. **0.4**

7.7 Cross bridge at Broad Canyon and stop at pullout for **STOP 2**. At 9:00 across the Rio Grande is a cliff composed of late

FIGURE 2.4. View eastward across the Rio Grande of the Eocene Palm Park Formation onlapped to the south by the latest Oligocene–early Miocene Hayner Ranch Formation.

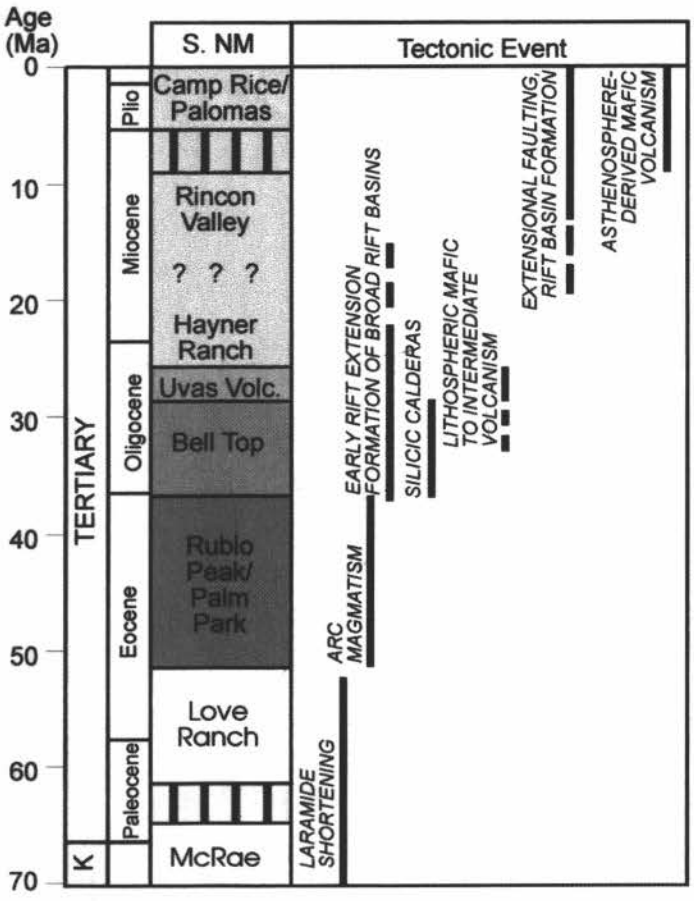

FIGURE 2.5. Cenozoic stratigraphic column and tectonic interpretations for south-central New Mexico.

Eocene andesitic lahars of the Palm Park Formation (Fig. 2.4). The northern part of the cliff displays a thin wedge of latest Oligocene–early Miocene conglomerate of the Hayner Ranch Formation that onlaps the Palm Park to the south.

Broad Canyon Foot Log for Stop 2

Cenozoic stratigraphy of south-central New Mexico records evidence of magmatic activity that accompanied tectonic events for the last 70 Ma, which permits the interpretation of mantle and crustal anatexis during Laramide shortening, the transition to Rio Grande rift extension, and continental rifting (Fig. 2.5). The traverse up Broad Canyon is designed to illustrate the early stage of structural evolution of the southern rift, and it provides an opportunity to examine geochemical evidence for changes in magma source regions and styles of volcanism during rifting. Stratigraphic units to be encountered include, in ascending order, the early Oligocene Bell Top Formation, the late Oligocene Uvas Basaltic Andesite, and the late Miocene Rincon Valley Formation, including the Selden Basalt (Fig. 2.5).

The late Eocene Palm Park and Rubio Peak Formations consist of calc-alkaline andesitic through rhyolitic lava flows, ash-flow tuffs, lahars, and associated volcaniclastic rocks that were erupted after Laramide shortening. The style of volcanism changed abruptly at about 37 Ma from intermediate composite cones dominated by lava flows to bimodal associations of silicic ash-flow tuffs and intercalated basaltic and basaltic andesite lava flows. The tuffs erupted during this time are part of the Bell Top Formation, which ranges in age from 35.7 to 28.6 Ma (McIntosh et al., 1991). Out-flow sheets collected in a half graben that developed during the early evolution

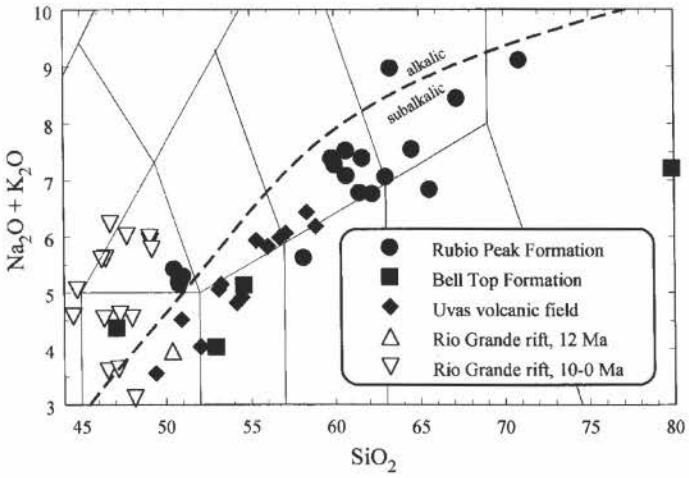

FIGURE 2.6. Total alkalis versus silica bivariate plot for post-Laramide Tertiary volcanic rocks of south-central New Mexico (N. J. McMillan, unpubl., 1998).

of the Rio Grande rift (Mack et al., 1994c). Overlying the uppermost ash-flow tuff of the Bell Top Formation (tuff 7; Vicks Peak Tuff) are the calc-alkaline basalts, basaltic andesites, and andesites of the Uvas Basaltic Andesite (28–26 Ma). Uvas volcanism marks the end of the first cycle of rift magmatism. Although extension continued for the next 16 Ma and basins were filled with about 6500 ft of sediment of the Hayner Ranch and Rincon Valley Formations, no volcanism is recorded in south-central New Mexico during this period. Volcanism resumed at 12 Ma at Hachita, followed by sporadic eruptions of single basalt flows and small volcanic centers as young as 4.8 ka (Anthony et al., this guidebook). The Selden Basalt, dated at 9.6 Ma (Seager et al., 1984), is an example of this late Cenozoic mafic volcanism.

Major geochemical shifts are recorded in the compositions of Cenozoic Rio Grande rift volcanic rocks (Figs. 2.6, 2.7, and 2.8). Rubio Peak, Bell Top, and Uvas lavas are mainly calc-alkaline, although the Rubio Peak basalts and one Bell Top basalt are weakly alkaline (Fig. 2.6). These Eocene through Oligocene volcanic rocks have low Ta and Nb concentrations, and exhibit incompatible trace element patterns similar to lavas produced in modern continental arcs (Fig. 2.7). They also have enriched Sr- and Nd-isotopic compositions (Fig. 2.8), with the most mafic lavas having (Nd values of +1, suggesting that they were derived from an enriched, probably lithospheric, mantle source and evolved by assimilation

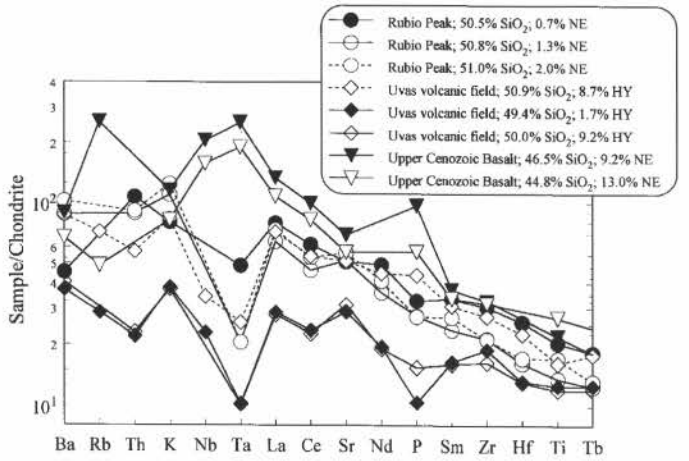

FIGURE 2.7. Chondrite-normalized (except Rb, K, and P) incompatible trace element patterns for Cenozoic basalts of south-central New Mexico. Normalization factors from Thompson (1982) (N. J. McMillan, unpubl., 1998).

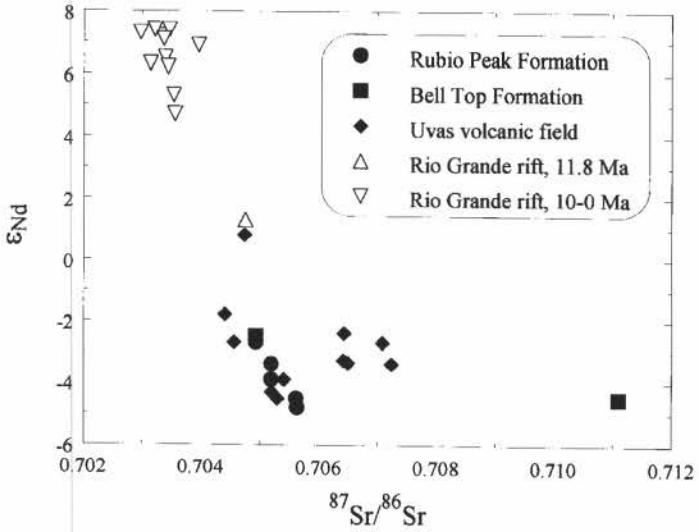

FIGURE 2.8. Sr and Nd isotope diagram for post-Laramide Tertiary volcanic rocks of south-central New Mexico (N. J. McMillan, unpubl., 1998).

and fractional crystallization in the crust. Upper Cenozoic basalts, in contrast, are dominantly alkaline (Fig. 2.6), have high Ta and Nb concentrations similar to young Basin and Range basalts and modern ocean island basalts (Fig. 2.7), and have relatively depleted Sr- and Nd-isotopic compositions (Fig. 2.8). These younger basalts are partial melts of convecting asthenosphere that melted by decompression when extension became great enough to allow sufficient asthenospheric upwelling.

Thus, the Cenozoic volcanic suite of south-central New Mexico provides evidence of two distinct styles of melting. Early in the evolution of the rift, hydrated lithospheric mantle melted due to extension and the addition of heat from the asthenosphere moving upward to replace the failed Farallon plate. As extension proceeded, the fusible parts of the lithosphere were removed by melting. Eventually, extension produced block-fault uplifts and basins, but neither lithosphere nor asthenosphere could melt. It was only when extension produced enough room for the asthenosphere to rise and experience decompression melting that the mafic volcanism commenced.

Mileage

0.0 **Follow the ranch road westward from the parking spot to the dam and walk along the crest of the dam to the south.**

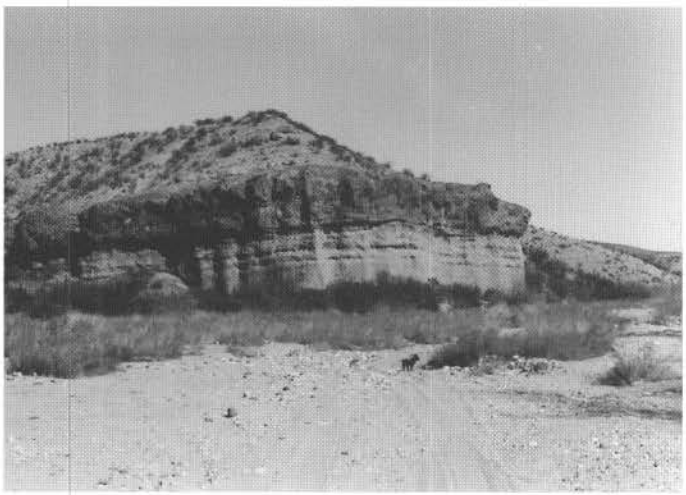

FIGURE 2.10. Outcrop of the Selden Basalt interbedded with conglomerates of the late Miocene Rincon Valley Formation at Foot Log Stop 1.

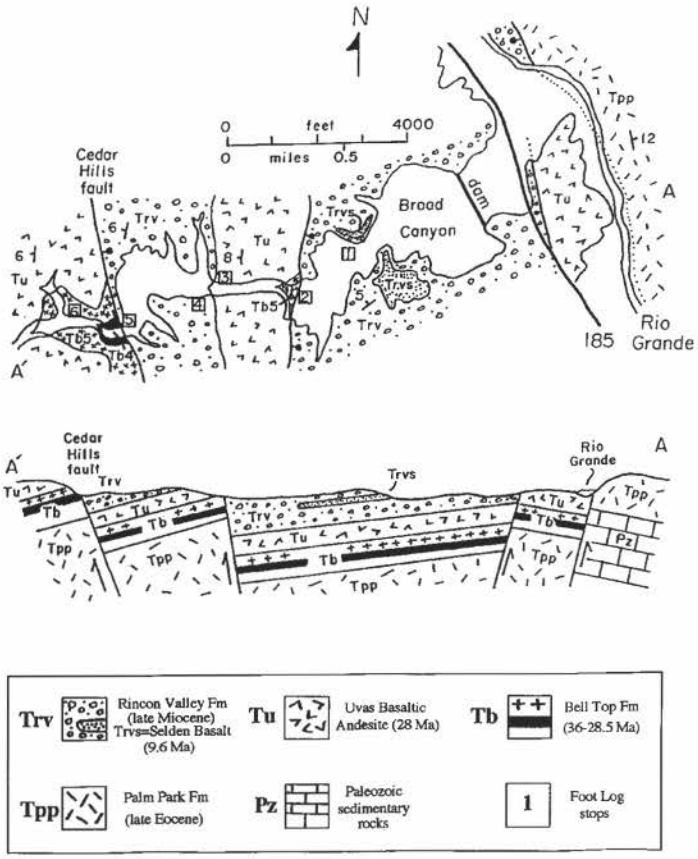

FIGURE 2.9. Generalized geologic map and foot log stops for Broad Canyon, adapted from Seager et al. (1975).

Descend into Broad Canyon, following the road to where the canyon narrows (Fig. 2.9). **1.0**

1.0 **FOOT LOG STOP 1**. Outcrops on both sides of the canyon belong to the late Miocene Rincon Valley Formation and consist of alluvial-fan conglomerates and the 9.6 Ma Selden Basalt (Figs. 2.10 and 2.11; Seager et al., 1984). **0.4**

1.4 **FOOT LOG STOP 2** is where the canyon narrows and turns northward, just beyond the old windmill (Fig. 2.12). At this site, a north-trending, east-dipping normal fault brings ash-flow tuff 5 of the Bell Top Formation in contact with the Rincon Valley Formation. This tuff has been dated by single-crystal sanidine $^{40}Ar/^{39}Ar$ analysis to be 34.8 Ma (McIntosh et al., 1991). Overlying ash-flow tuff 5 are lava flows of the Uvas Basaltic Andesite (28 Ma; Seager et al., 1984). **0.3**

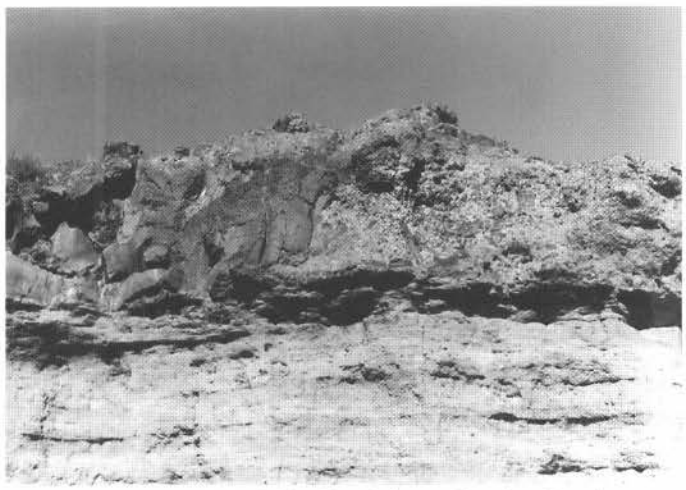

FIGURE 2.11. Base of the Selden Basalt flow at Foot Log Stop 1.

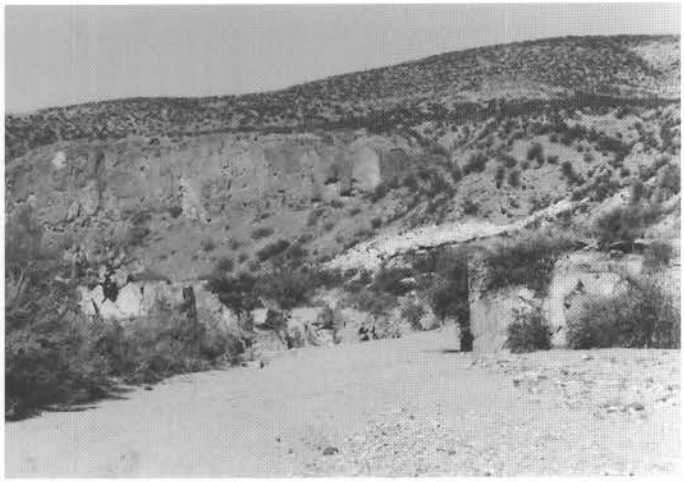

FIGURE 2.12. Ash-flow tuff 5 exposed at arroyo level at Foot Log Stop 2. Dark cliffs belong to the Uvas Basaltic Andesite.

FIGURE 2.13. View to the north of exhumed cinder cone of the Uvas Basaltic Andesite at Foot Log Stop 3.

1.7 At **FOOT LOG STOP 3**, the canyon widens and turns northward. At arroyo level is a cinder cone in the Uvas Basaltic Andesite (Figs. 2.13, 2.14, and 2.15). Dips to the east, opposite that of the regional tectonic dip, suggest that this is the eastern margin of the cinder cone. The lava flow under the cinder cone contains olivine crystals altered to iddingsite. Although many petrologists consider iddingsite to be an alteration product of olivine, mafic Uvas lavas contain magmatic iddingsite. Olivine cores are rimmed by a region of bright rust-red iddingsite, which is in turn rimmed by fresh olivine. The outermost olivine is always more iron-rich than the cores, demonstrating that the iddingsite crystallized from the magma at high temperatures. The iddingsite is a mixture of cristobalite, orthopyroxene, $Fe_2O_3 1.2H_2O$, and maghemite or hematite, similar to the results of Goff (1996). Electron microprobe analyses indicate that the bulk composition of the iddingsite correlates with the bulk composition of the host magma. K_2O contents in iddingsite are higher in moderate-K_2O lavas than in low-K_2O lavas. The iddingsite is extremely fine-grained; the potassium-bearing mineral has not yet been identified. However, Boyers et al. (1996) concluded that the magmatic iddingsite formed by the reaction of olivine phenocrysts, water, and magma at magmatic temperatures. **0.05**

1.75 **FOOT LOG STOP 4**. The late Miocene Rincon Valley Formation unconformably overlies the Uvas Basaltic Andesite (Figs. 2.16 and 2.17). At this location, the Rincon Valley Formation consists of alluvial-fan conglomerates. Initially, the Rincon Valley conglomerates filled paleovalleys cut into the Uvas Basaltic Andesite and consequently are coarse and composed almost exclusively of Uvas clasts. Subsequently, the Rincon Valley conglomerates were deposited on the midfan to distal fan reaches of broad alluvial fans whose source was to the east and southeast (Fig. 2.18). These fans occupied the hanging wall dip slope of a half graben, whose footwall was the Sierra de las Uvas. The hanging wall-derived conglomerates contain distinctive clasts of flow-banded rhyolite and contact metamorphosed Abo and Hueco clasts which are only exposed to the south and east and are not present in the Sierra de las Uvas to the west. The latest Oligocene to early Miocene Hayner Ranch Formation is not present here, because this area was part of the hanging wall uplift during Hayner Ranch time (Fig. 2.19). Broad Canyon makes a large, northerly bend beyond this point, but proceed due west across the low inset terrace toward the steep cliff. **0.3**

2.05 **FOOT LOG STOP 5** is at the base of the steep cliff, which marks the location of the Cedar Hills fault, a north-trending, east-dipping normal fault with ash-flow tuffs 4 and 5 and the Uvas Basaltic Andesite on the footwall and the Rincon Valley Formation on the hanging wall (Figs. 2.20 and 2.21). The Cedar Hills and other faults in this area are positioned

FIGURE 2.14. View to the east of the base of the exhumed cinder cone of the Uvas Basaltic Andesite at Foot Log Stop 3.

FIGURE 2.15. Cemented cinders of the exhumed cinder cone of the Uvas Basaltic Andesite at Foot Log Stop 3.

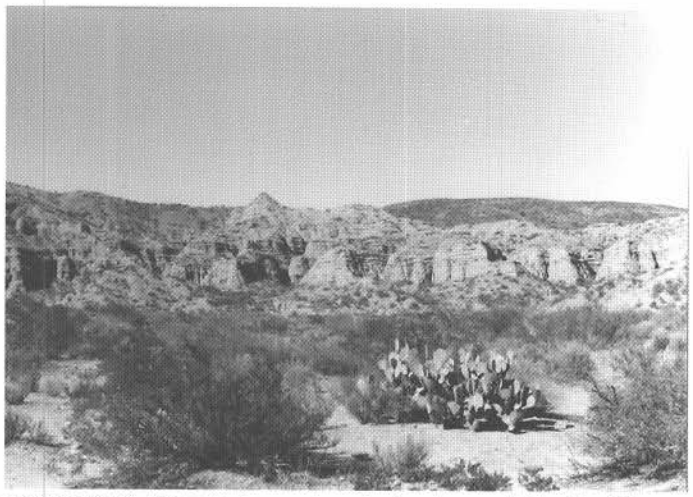

FIGURE 2.16. View to the northwest of outcrops of the late Miocene Rincon Valley Formation at Foot Log Stop 4.

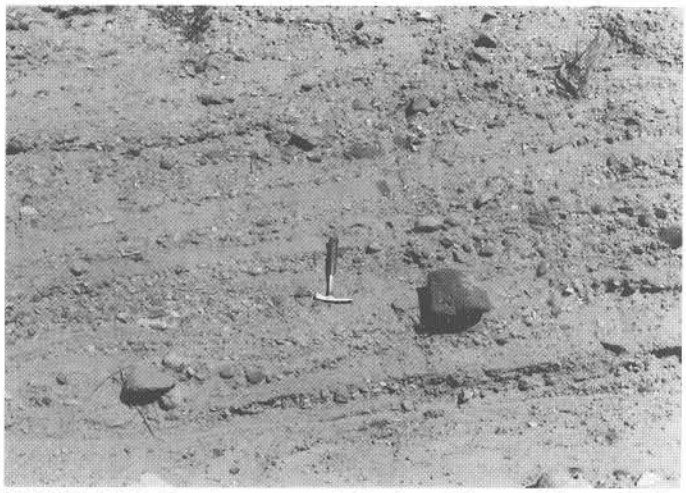

FIGURE 2.17. Conglomerates of the late Miocene Rincon Valley Formation deposited in a midfan or distal fan setting at Foot Log Stop 4.

within the Cedar Hills transfer zone, which transfers strain from the West Robledo fault to the Ward Tank fault (Fig. 2.22; Mack and Seager, 1995). The style of this transfer zone is a broad, north-trending arch whose crest collapsed into a graben along a series of north-trending normal faults that dip toward the axis of the arch. The Cedar Hills fault is the largest fault west of the crest of the arch. Proceed up the canyon to where it narrows (Fig. 2.23). Ash-flow tuff 4 is exposed at arroyo level in the narrow canyon (Fig. 2.24), and has been dated by single-crystal sanidine $^{40}Ar/^{39}Ar$ at 35.0 Ma (McIntosh et al., 1991). **0.1**

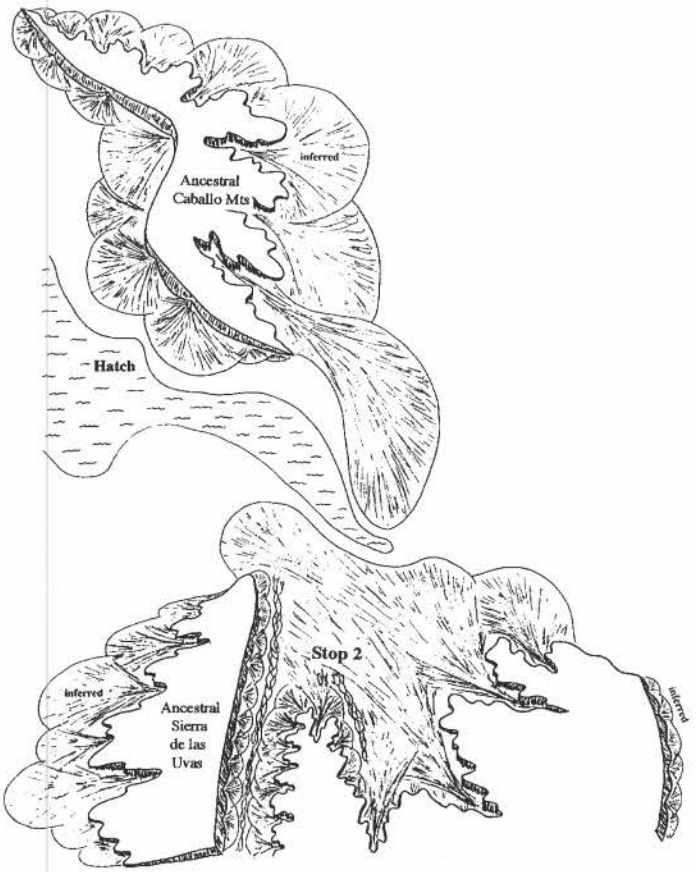

FIGURE 2.18. Paleogeographic map during deposition of the late Miocene Rincon Valley Formation in south-central New Mexico, adapted from Mack et al. (1994b). Stop 2 refers to the approximate location of Broad Canyon.

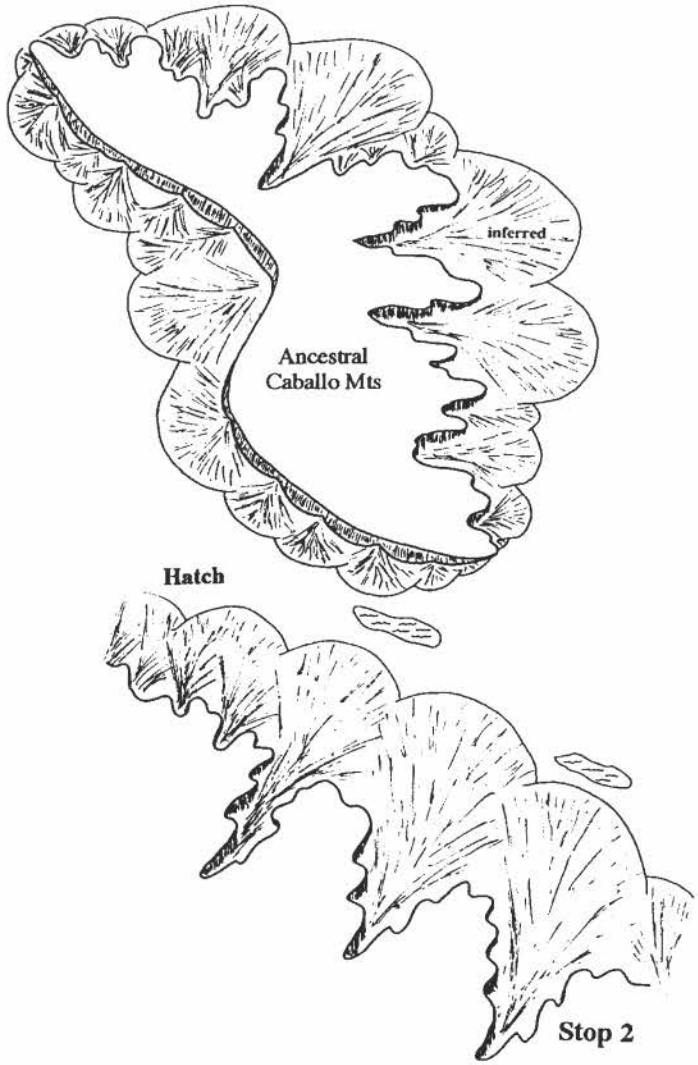

FIGURE 2.19. Paleogeographic map during deposition of the latest Oligocene–early Miocene Hayner Ranch Formation in south-central New Mexico, adapted from Mack et al. (1994b). Stop 2 refers to the approximate location of Broad Canyon.

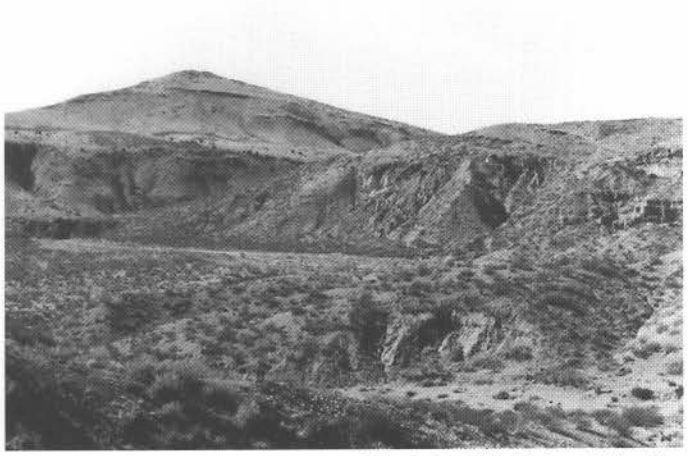

FIGURE 2.20. View to the west toward the Cedar Hills fault and Foot Log Stop 5.

FIGURE 2.21. View to the northwest of the Cedar Hills normal fault, which places the Bell Top Formation and overlying Uvas Basaltic Andesite on the footwall against the Rincon Valley Formation (light-colored rocks on right side of photo) on the hanging wall.

2.15 **FOOT LOG STOP 6**. Where the canyon widens, there is a good view of the light-colored cliff of ash-flow tuff 5 (Figs. 2.25 and 2.26). Exposed at several locations at the base of the cliff are Native American petroglyphs (Fig. 2.27). **2.15**

End of Traverse. Retrace route to parking spot.

Continuation of Road Log.

8.4 View of Ash Mesa at 11:00 (Fig. 2.28), which consists of the late Miocene Rincon Valley Formation overlain by inset sands, gravel, and the Lava Creek B fallout ash derived from the Yellowstone caldera (Seager et al., 1975; Mack et al., 1993). **1.9**

10.3 At 1:00 is the flat-topped San Diego Mountain (Fig. 2.29), at which is exposed about 5000 ft of latest Oligocene and Miocene basin-fill sedimentary rocks of the Hayner Ranch and Rincon Valley Formations (Seager et al., 1971; Mack et al., 1994b). At 2:00 is a steep brown cliff immediately across the Rio Grande that consists of proximal alluvial-fan conglomerates of the latest Oligocene–early Miocene Hayner Ranch Formation (Fig. 2.30). At 3:00 are the northern end of the Selden Hills, where the Hayner Ranch Formation onlaps southward the Eocene Palm Park Formation (Fig. 2.31). **0.9**

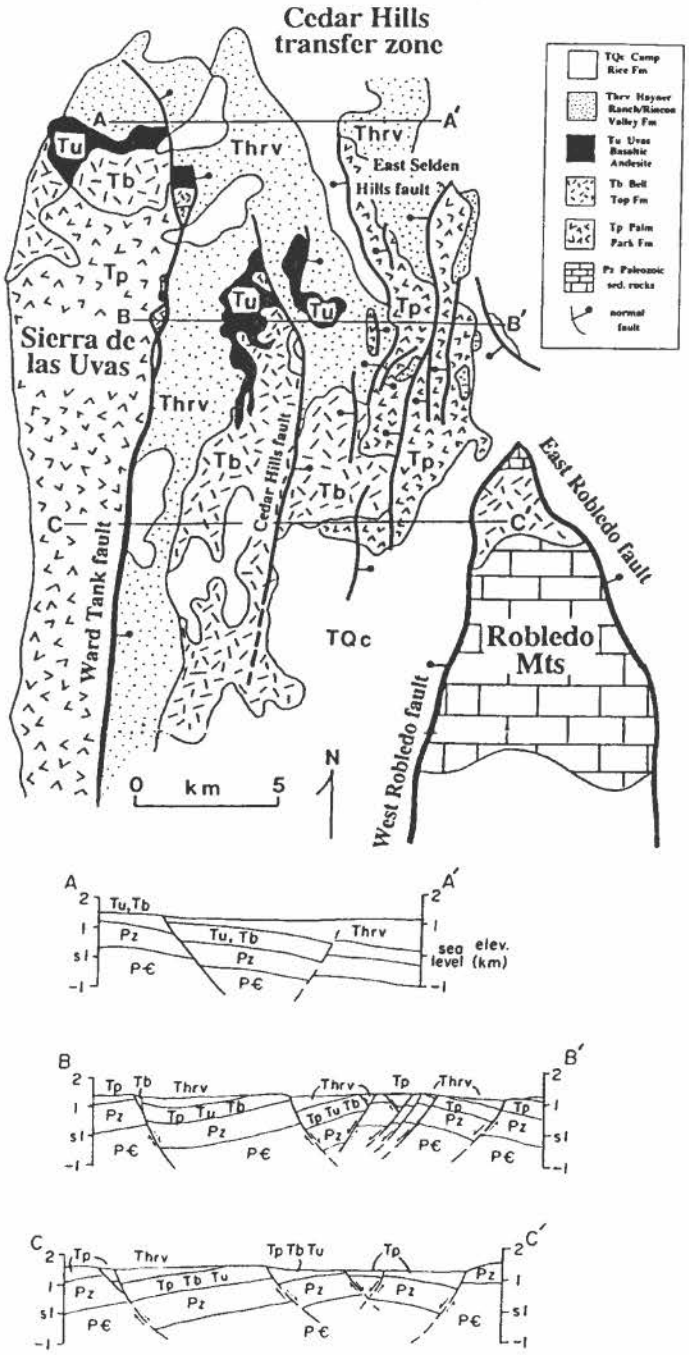

FIGURE 2.22. Geologic map and cross sections of the Cedar Hills transfer zone, adapted from Mack and Seager (1995). Broad Canyon Foot Log Stop 5 is at the base of the Cedar Hills fault.

11.2 Leaving Selden Canyon. San Diego Mountain is visible at 3:00 (Fig. 2.32). **1.9**

13.1 Border Check Station. **Proceed north on NM-185**. Bluffs at 9:00 are underlain by the late Miocene Rincon Valley Formation. Low mesa at 3:00 in the far distance is the La Mesa geomorphic surface, which represents the constructional top of the axial-fluvial facies of the Plio–Pleistocene Camp Rice Formation. **4.9**

18.0 **Turn right onto NM-140** toward the town of Rincon. At 11:00 is Red House Mountain and at 12:00 are the Rincon Hills. **0.4**

18.4 The highway crosses the Rio Grande. **0.9**

19.3 Cross railroad tracks. **0.9**

FIGURE 2.23. Narrow segment of Broad Canyon cut into ash-flow tuff 4 of the Bell Top Formation.

FIGURE 2.24. Outcrop view of ash-flow tuff 4 of the Bell Top Formation. Dark, irregular features are flattened pumice clasts. Hammer is 10 in. long.

FIGURE 2.25. View to the west of ash-flow tuff 4 overlain by ash-flow tuff 5 of the Bell Top Formation.

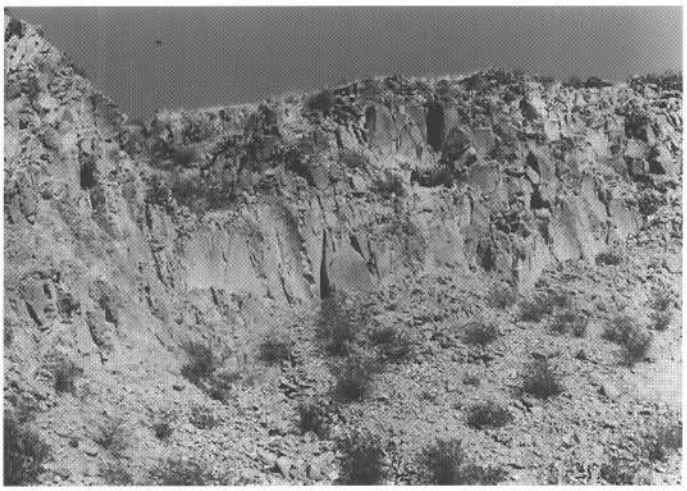

FIGURE 2.26. Cliff of ash-flow tuff 5 of the Bell Top Formation exposed at Foot Log Stop 6.

FIGURE 2.27. Native American petroglyphs chipped into ash-flow tuff 5 of the Bell Top Formation at Foot Log Stop 6.

FIGURE 2.28. Ash Mesa, as viewed from NM-185. Near the top of the mesa is an exposure of the Lava Creek B ash derived from the 0.61 Ma eruption of the Yellowstone caldera (Seager et al., 1975).

FIGURE 2.29. San Diego Mountain (Tonuco uplift) as viewed from NM-185.

FIGURE 2.30. View to the east across the Rio Grande from NM-185 of coarse conglomerates of the latest Oligocene–early Miocene Hayner Ranch Formation.

FIGURE 2.31. View to the east across the Rio Grande from NM-185 of the Hayner Ranch Formation, which progressively onlaps the Palm Park Formation to the south.

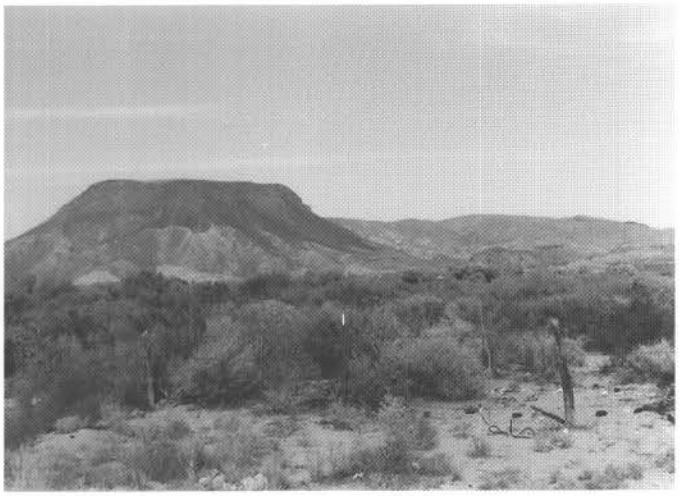

FIGURE 2.32. View to the east from NM-185 of San Diego Mountain.

FIGURE 2.33. View northward from the Upham Road of the Caballo Mountains.

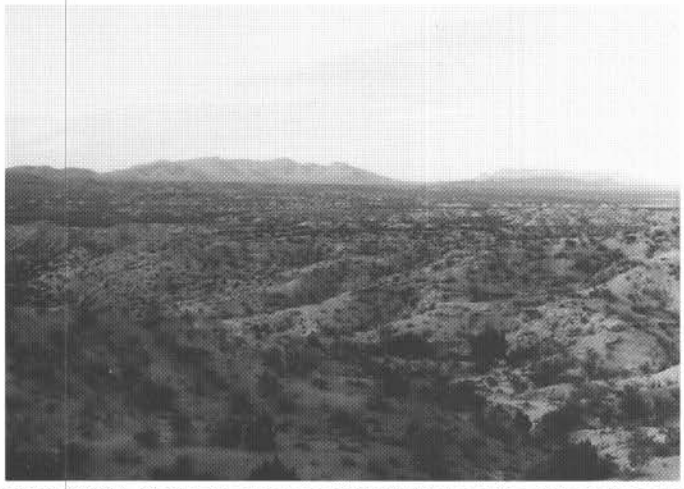

FIGURE 2.34. Badlands exposures of fluvial facies of the Plio–Pleistocene Camp Rice Formation at Stop 3. Caballo Mountains in the background.

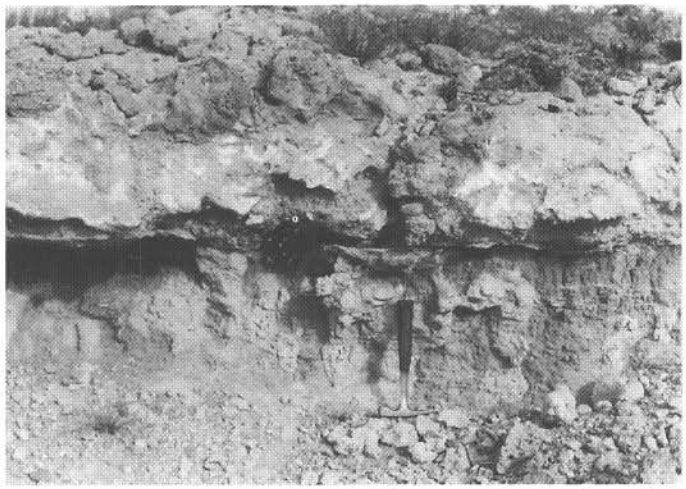

FIGURE 2.35. Calcic paleosol behind hammer; fluvial facies of the Plio–Pleistocene Camp Rice Formation, Stop 3.

19.7 Enter town of Rincon. **0.4**

20.4 **Turn left onto I-25**—south toward Las Cruces. Highway crosses bridge over Rincon arroyo and ascends toward the La Mesa surface. Roadcuts are the axial-fluvial facies of the Plio–Pleistocene Camp Rice Formation. **1.8**

23.2 **Turn off I-25** at Upham exit (exit 32). **Turn left at stop sign** and go under overpass. Cross cattle guard and proceed on dirt road (Fig. 2.33). At 11:00 are the Rincon Hills; at 12:00 is Red House Mountain; at 1:00 are the Caballo Mountains; at 2:00 is the Point of Rocks.

24.5 **Veer right at Y junction, following E72. 1.0**

25.5 **Pull over where steep gully approaches road from the west** for **STOP 3**. Walk 0.25 mi westward along the southern margin of the canyon to where a promontory juts northwestward into canyon. Follow path over the edge of the La Mesa surface to a sandy bench about 30 ft below.

Exposed beneath the La Mesa surface is the axial-fluvial facies of the Plio–Pleistocene Camp Rice Formation, which consists of interbedded channel pebbly sands and floodplain very fine sand and red mudstone (Fig. 2.34). Many of the floodplain sediments contain calcic paleosols, which commonly consist of an argillic B horizon overlying a stage II nodular calcic B horizon (Fig. 2.35; Mack and James, 1992). Stable oxygen and carbon isotopes of the pedogenic carbonate have been used by Mack et al. (1994d) as paleoclimate indicators (Fig. 2.36). These data suggest that throughout the history of deposition of the Camp Rice Formation the region became progressively hotter and/or drier.

The La Mesa surface is directly underlain by a stage V petrocalcic paleosol, characterized by a several foot-thick, well indurated K horizon with a laminar cap and well-developed brecciation and pisoliths (Fig. 2.37; Gile et al., 1981).

Also present within the Camp Rice Formation at this stop is a 1.5-ft-thick pumice-clast conglomerate (Figs. 2.38 and 2.39). The pumice in this bed has been dated by single-crystal sanidine $^{40}Ar/^{39}Ar$ analysis at 1.59 Ma (Mack et al., 1996). This age, the coarse size of the pumice clasts, and the paucity of other clast types suggest that the pumice conglomerate was transported as a giant flood following the lower Bandelier eruption in the Jemez volcanic field. Pumice conglomerates similar in age to the one exposed here have been found near I-10 west of Las Cruces, at La Union, and on the Jornada Experimental Station north of the Doña Ana Mountains. In addition, four other pumice-clast conglomerates have been found in southern New Mexico, ranging in age from 3.12 Ma near Hatch, 2.22 Ma at the Doña Ana Range Camp, 1.84 Ma at Berino Tank, and 1.3 Ma at La Union (Mack et al., 1996).

The Camp Rice and Palomas Formations in southern New Mexico have been dated and correlated using reversal magnetostratigraphy (Mack et al., 1993; Leeder et al., 1996).

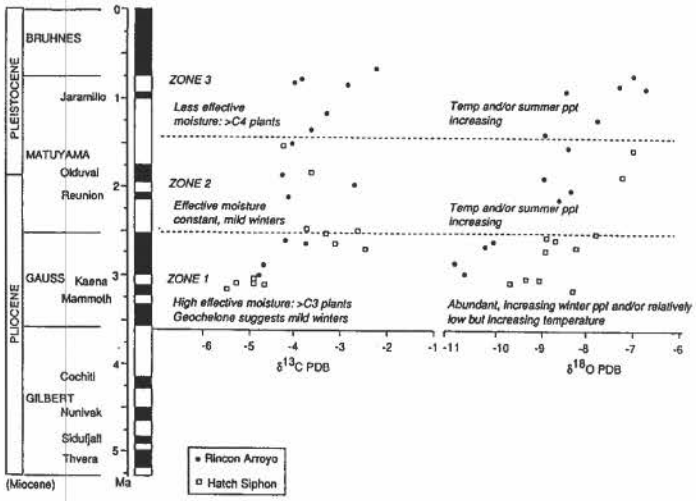

FIGURE 2.36. Stable oxygen and carbon isotope data from pedogenic carbonate of the Plio–Pleistocene Camp Rice Formation, adapted from Mack et al. (1994d).

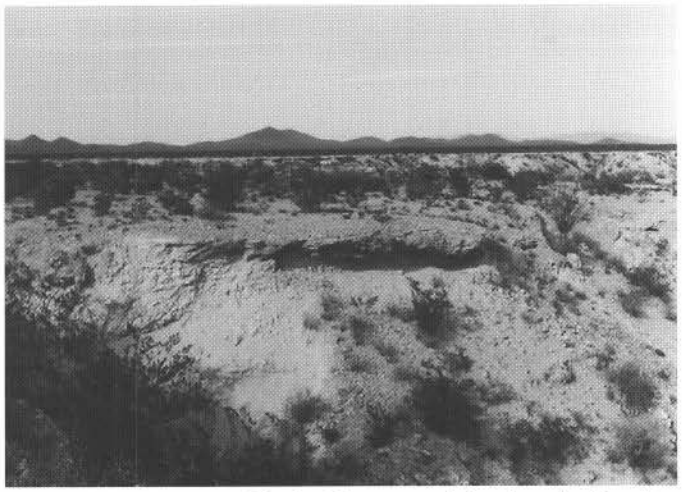

FIGURE 2.37. Exposure of the La Mesa petrocalcic paleosol at Stop 3.

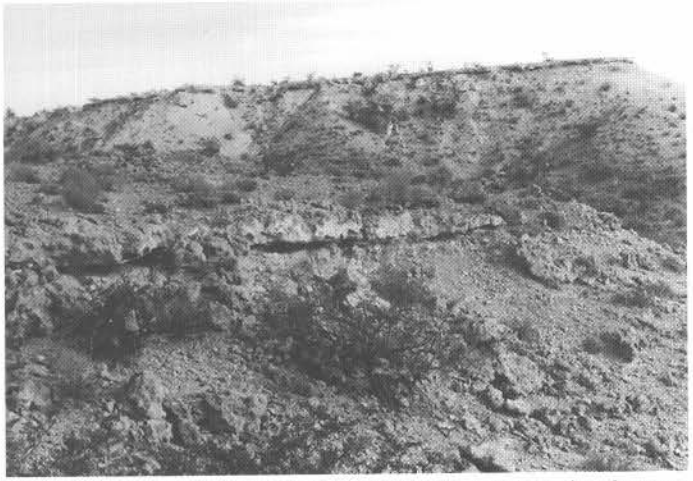

FIGURE 2.38. Ledge in center of photo is the 1.6 Ma pumice-clast conglomerate within the fluvial facies of the Plio–Pleistocene Camp Rice Formation. Mesa surface corresponds to the constructional top of the Camp Rice Formation (La Mesa surface).

FIGURE 2.39. Close up of the 1.6 Ma pumice-clast conglomerate, which is presumably derived from the lower Bandelier eruption (Mack et al., 1996).

Radioisotopically dated pumice-clast conglomerates and fallout ashes are used to tie the magnetostratigraphic sections to the geopolarity-reversal time scale. The section at Rincon Arroyo, just 1 mi south of this stop, contains approximately 165 ft of Gauss-age sediment, including one subchron, and about 150 ft of Matuyama-age sediment (Fig. 2.40). The Matuyama part of the section contains all four subchrons and can be constrained by the presence of the 1.59 Ma pumice conglomerate. The oldest section dated using magnetostratigraphy is near Garfield, where fluvial sediment belonging to the Gilbert chron is as old as 4.9 Ma (Leeder et al., 1996). The age of the top of the Camp Rice

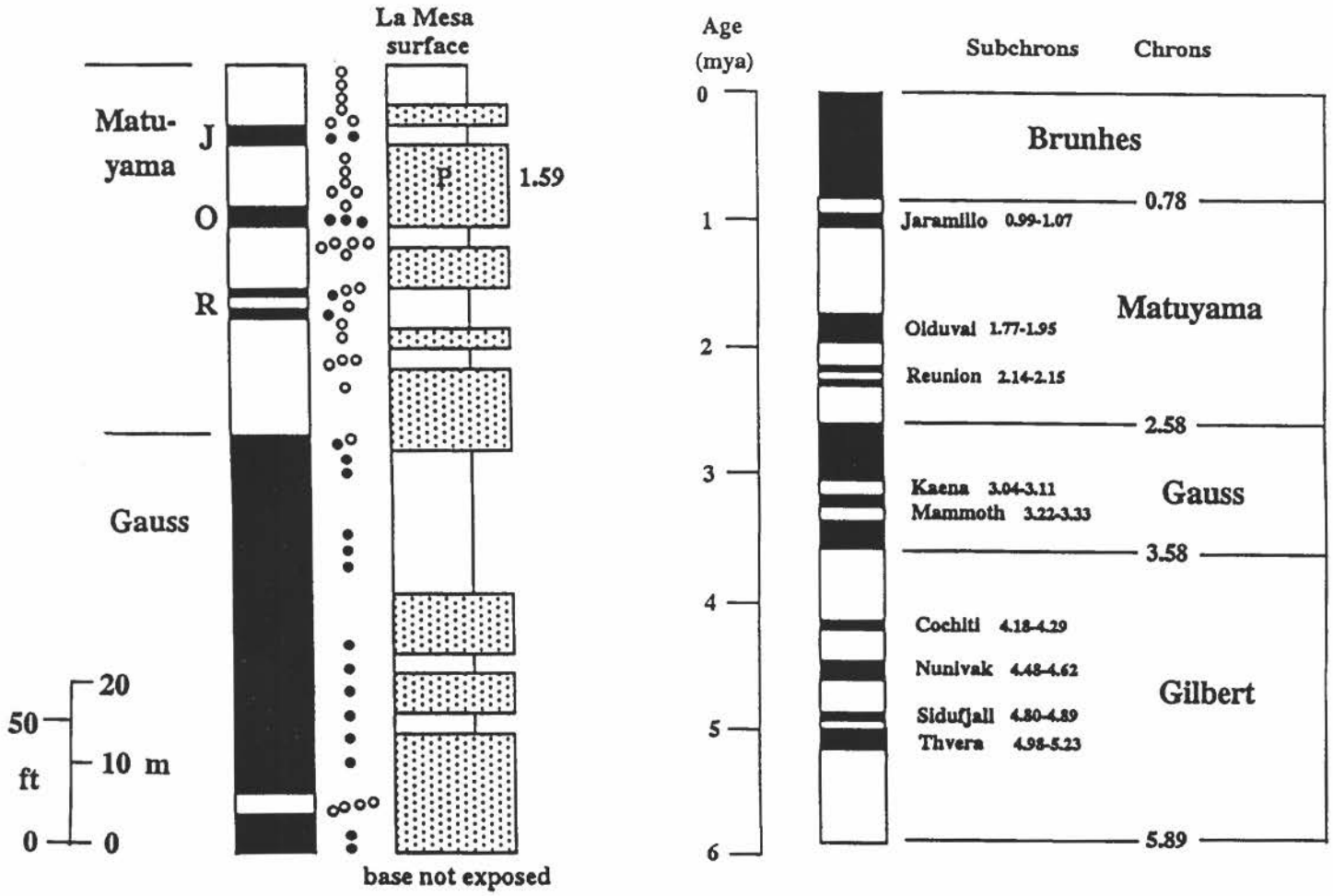

FIGURE 2.40. Magnetostratigraphy of the Camp Rice Formation at Rincon Arroyo (Mack et al., 1993, 1996). "P" refers to pumice-clast conglomerate and "1.59" is its radioisotopic age in millions of years. J = Jaramillo subchron; O = Olduvai subchron; R = Reunion subchrons. To the right is the polarity reversal time scale based on Berggren et al. (1995).

and Palomas Formations, which also corresponds to the age of the La Mesa surface, can also be constrained by reversal magnetostratigraphy to be near or at the Matuyama-Brunhes chron boundary, approximately 0.78 Ma (Mack et al., 1993, 1996). **0.25**

EARLY PLEISTOCENE (EARLY IRVINGTONIAN) CO-OCCURRENCE OF THE PROBOSCIDEANS *CUVIERONIUS, STEGOMASTODON*, AND *MAMMUTHUS* AT TORTUGAS MOUNTAIN, DOÑA ANA COUNTY, NEW MEXICO

Spencer G. Lucas[1], Gary S. Morgan[1], and Greg H. Mack[2]

[1]New Mexico Museum of Natural History, 1801 Mountain Road NW, Albuquerque, NM 87104; [2]Department of Geological Sciences, New Mexico State University, Las Cruces, NM 88003

In western North America during the late Pliocene and/or early Pleistocene, two proboscideans—the mammoth *Mammuthus* and the gomphothere *Stegomastodon*—were common, whereas the two, typically Central America gomphotheres *Cuvieronius*, and *Rhynchotherium* were relatively uncommon. Three of these proboscideans—*Cuvieronius*, *Stegomastodon*, and *Mammuthus*—co-occur in the Camp Rice Formation at Tortugas Mountain, Doña Ana County, and this co-occurrence establishes an age of early Irvingtonian.

The Tortugas Mountain locality, NMMNH locality 3537, is a gravel pit located at UTM 3574500N, 339350E, Zone 13. This pit exposes axial river gravels and sands of an ancestral Rio Grande, deposits assigned to the upper part of the Camp Rice Formation.

The *Stegomastodon* from NMMNH locality 3537 is NMSUM (New Mexico State University Museum, Las Cruces) 75.2.4, a palate with left and right M^{2-3} described by Vanderhill (1986). The molar crowns of this specimen are extremely complex, and M^3 has six lophs, indicating it is a very derived specimen of *Stegomastodon mirificus sensu* Kurtén and Anderson (1980). This *Stegomastodon* is much more advanced evolutionarily than the early Blancan *Stegomastodon* from the Palomas Formation near Truth or Consequences described by Lucas and Oakes (1986).

The *Cuvieronius* specimen from NMMNH locality 3537 is NMSUM 79.17.1, a right dentary with incomplete M_2 and a complete M_3. This specimen shows several features characteristic of *Cuvieronius*: the jaw lacks tusks and has a short symphysis, and the M_3 is bunolophodont with 4 lophids, single trefoils and slightly alternating cuspids between the lophids. Therefore, we identify NMSUM 79.17.1 as *Cuvieronius* sp. A nearby gravel pit on what is now east Lohman Avenue in Las Cruces also produced specimens of *Cuvieronius* and *Mammuthus* from the same stratigraphic level as NMMNH locality 3537 (Hawley et al., 1969; Vanderhill, 1986).

Specimens of *Mammuthus* from NMMNH locality 3537 consist of a left M_3 (NMSUM 140), a right M^2 (NMSUM 139) and an incomplete left M^3 (NMSUM 141). The M_3 has at least 17 plates, is 300+ mm long, 78 mm wide, and it has a plate ratio (number of plates per 100 mm) of 7, an average plate thickness of 9.1 and an average enamel thickness of 3.2. The M^2 has at least 13 plates, is 230 mm long, 94 mm wide, and it has a plate ratio of 6, average plate thickness of 11.2 and average enamel thickness of 3.4. The incomplete left M^3 is 98 mm wide, and it has a plate ratio of 7, average plate thickness of 12.2 and an average enamel thickness of 3.2. All of these measurements are well within the range of measurements Madden (1981, 1995) lists for *Mammuthus imperator*, to which we assign the Tortugas Mountain specimens. *M. imperator* is also known from several other sites in New Mexico (Lucas and Effinger, 1991; Lucas et al., 1993).

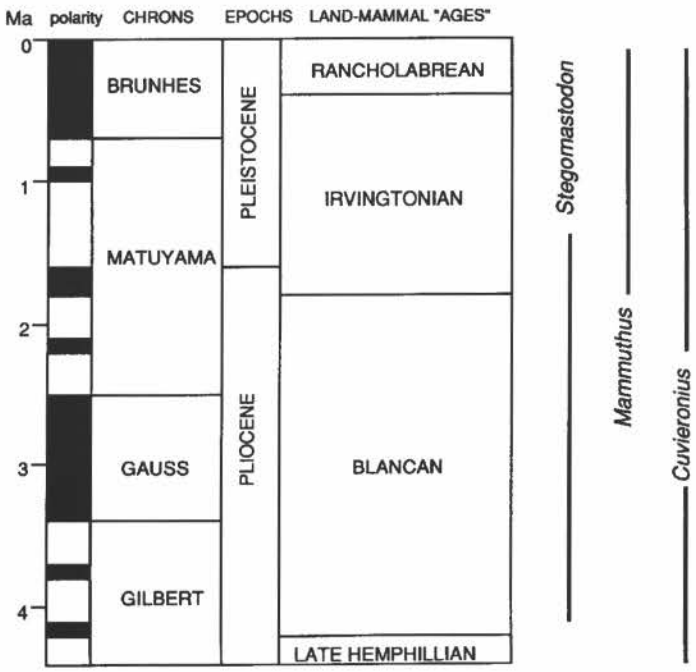

FIGURE 2.41. Temporal distribution of the three proboscidean genera found in the gravel pit at Tortugas Mountain.

In North America, *Stegomastodon* has a temporal range of Blancan through early Irvingtonian, *Mammuthus* ranges from the late early Irvingtonian (about 1.6 Ma) through the Rancholabrean, and *Cuvieronius* has a spotty record from the late Hemphillian (questionable records) through the Rancholabrean (Fig. 2.41). Thus, the Tortugas Mountain co-occurrence of these proboscideans is early Irvingtonian. This is a relatively rare record of the co-occurrence of these genera. One of the few other records in western North America is in the Seymour Formation in the Texas Panhandle where *Stegomastodon* and *Mammuthus* co-occur in an early Irvingtonian fauna (Hibbard and Dalquest, 1966; Schultz, 1984).

End of traverse. Retrace route to parking spot and back to Las Cruces.